Research Article | Vol. 14, No. 9 / 1 Sep 2023 / Biomedical Optics Express 4901
Biomedical Optics EXPRESS

Non-invasive method for assessment of inflammation

I. FINE,[1,*] A. KAMINSKY,[1] L. SHENKMAN,[1] AND M. AGBARIA[2]

[1]Elfi-Tech Ltd., 2 Prof. Bergman St., Science Park, 76705 Rehovot, Israel
[2]Clalit Service Shaked Unit, Israel
[*]Ilyafine@elfi-tech.com

Abstract: This article explores the potential of non-invasive measurement for elevated levels of erythrocyte aggregation *in vivo*, which have been correlated with a higher risk of inflammatory processes. The study proposes utilizing a dynamic light scattering approach to measure aggregability. The sensor modules, referred to as "mDLS," comprise VCSEL and two photodiodes. Two of these modules are placed on an inflatable transparent cuff, which is then fitted to the subject's finger root, with one sensor module positioned on each side. By temporarily halting blood flow for one minute using over-systolic inflation of the cuff, signals from both sensors are recorded. The study involved three distinct groups of subjects: a control group consisting of 65 individuals, a group of 29 hospitalized COVID-19 patients, and a group of 34 hospitalized patients with inflammatory diseases. Through experimental results, significant differences in signal kinetic behavior were observed between the control group and the two other groups. These differences were attributed to the rate of red blood cell (RBC) aggregation, which is closely associated with inflammation. Overall, the study emphasizes the potential of non-invasive diagnostic tools in evaluating inflammatory processes by analyzing RBC aggregation.

1. Introduction

RBC aggregation, also known as rouleaux formation, refers to the clumping of red blood cells (RBCs) when they are in proximity. This phenomenon is primarily determined by various constituents present in the blood plasma and is a reversible process [1]. When appropriate forces are applied, the aggregated RBCs disperse from each other. Several blood plasma constituents affect the process of RBC aggregation, including fibrinogen, which is an important factor in red blood cell aggregation, as it promotes the formation of bridges between cells. Some immunoglobulins, such as IgM, have been found to promote red blood cell aggregation. Environmental conditions also play an important role in RBC aggregation, such as the presence of electrolytes like sodium and potassium, which can affect the degree of red blood cell aggregation. Most of the factors mentioned above are related also to inflammation. Therefore, the degree of RBC aggregation is a crucial marker for characterizing the development of inflammatory processes in humans [2,3].

There is a direct relationship between RBC aggregation and the erythrocyte sedimentation rate (ESR) [4,5], which measures the rate at which red blood cells settle to the bottom of a test tube over time. These techniques rely on the well-known fact that when RBCs are aggregated, they settle more quickly. ESR is used as an inflammation marker [6]. Another widely recognized inflammation marker is the level of C-reactive protein (CRP) in the blood. Elevated levels of CRP are associated with several inflammatory conditions. Studies have shown that CRP, RBC aggregation rate and ESR are positively correlated, implying that an increase in one marker is often accompanied by an increase in the other [7]. In the study of Nader et al. [8], blood hyper-viscosity and RBC hyper-aggregation were demonstrated in a large cohort of patients with COVID-19, and associations with clinical outcomes were described. However, it is important to note that RBC aggregation is just one of many markers used to evaluate inflammation. It is often

#494637 https://doi.org/10.1364/BOE.494637
Journal © 2023 Received 2 May 2023; revised 8 Aug 2023; accepted 21 Aug 2023; published 25 Aug 2023

Biomedical Optics EXPRESS

used in conjunction with other clinical and laboratory parameters to provide a comprehensive assessment of the inflammatory response. The presence of other factors, such as medications or underlying medical conditions, can influence RBC aggregation independently of inflammation.

To measure the tendency of erythrocyte aggregation, the method of mechanical disruption of the bonds between them is often used, followed by observing the rate of the aggregation process. This method is called erythrocyte aggregometry. The process begins with the disruption of bonds between erythrocytes, for example, by shaking or agitating the cuvette containing the blood sample. Then, after the bonds are disrupted, erythrocytes start to form aggregates by sticking together. The rate of the aggregation process can be determined by observing changes in light scattering or other optical characteristics of the sample under consideration. [9,10,11,12]. The most effective way to break these bonds is to generate sufficiently significant shear forces. For instance, in the Laser-assisted Optical Rotational Cell Analyzer (LORCA), changes in light transmission through a blood sample are measured as RBCs aggregate under controlled shear conditions [13]. Laser aggregometry can provide objective measurements of red blood cell aggregation, such as aggregation indices or aggregation kinetics, which are useful for research purposes and clinical assessments of blood rheology. Another well-known *in vivo* method that can be used for the assessment of the RBC aggregation is capillaroscopy. Capillaroscopy is a non-invasive imaging technique that allows for the direct visualization of microcirculation in the capillaries. By observing the behavior and arrangement of red blood cells within capillaries, capillaroscopy can provide qualitative information about the degree of red blood cell aggregation [14].

Although various *in vitro* methods exist for measuring red blood cells aggregation, non-invasive assessment of blood aggregability remains a challenging task. In order to put forth an alternative methodology for the non-invasive assessment of red blood cell aggregation, it is imperative to take into account any observable phenomena associated with this process. In recent studies [16,17], a novel hypothesis was introduced, proposing that the pulsatile signal observed in peripheral photoplethysmography (PPG) is indicative of the dynamic processes of erythrocyte aggregation and disaggregation occurring within the blood vessels. It was suggested that the pulsatile nature of vascular blood flow leads to fluctuation of shear forces, which results in the modulation of the average size of red blood cells [15]. However, evaluating the aggregability of blood solely from a pulse signal is a complex task, primarily due to the influence of shear forces, which are contingent upon the velocity of blood flow and the dimensions of the blood vessels. Consequently, it appears that the most straightforward approach to observe aggregation is to mitigate the effects of shear forces by arresting their action. By halting the blood flow and consequently neutralizing shear forces, the growth of aggregates can proceed undisturbed, thereby enabling the kinetics of the optical signal measurement to be exclusively governed by the rate of aggregation. In this manner, any external factors that may influence the measurement are effectively eliminated, allowing for a more accurate assessment of the aggregation process. To cease the blood flow, it is possible to apply over-systolic pressure to the specific location under examination, such as the finger. This approach, which can be readily implemented in vivo, involves measuring the transmission of light through the finger and has been extensively discussed in various previous studies and reports [18,19,20]. In these studies, in order to experimentally validate the concept, an array of LEDs was positioned on one side of the finger base, while the detector was positioned on the opposite side. This setup allowed for the measurement of visible and near-infrared light transmission through the finger, thereby enabling the assessment of the proposed idea. To induce the desired effect, a pneumatic cuff was utilized to apply over-systolic to the measurement site. This application of pressure led to a swift and significant augmentation in light transmission through the base of the finger. The observed change in the signal was attributed to a decrease in light scattering on erythrocytes due to the process of their aggregation. Nevertheless, it is crucial to acknowledge that while this method has been successfully employed

Biomedical Optics EXPRESS

for the calculation of various blood parameters, such as arterial blood oxygen saturation and hematocrit levels, the investigation of blood aggregability kinetics remains largely unexplored within this context. Employing post-occlusion optical signal kinetics presents a notable challenge due to different factors that impact the measured optical signal. These factors encompass not only the complex phenomena of multiple scattering and light absorption but also various aspects such as fluctuations in blood oxygen levels, variations in blood volume, and changes in the transparency of skin tissue. These combined factors contribute to the intricacy of accurately interpreting the optical signal, necessitating careful consideration and rigorous analysis in order to obtain meaningful insights.

In this work, we use an approach based on dynamic light scattering (DLS). DLS is a technique that utilizes the fluctuations of scattered light intensity to determine the size and motion of particles or molecules in a solution or suspensions [21]. One of the most important advantages of the DLS methodology is that in the geometry of single light scattering, the obtained signal does not depend on the properties of the skin, absorption of hemoglobin, and other aforementioned factors. The principle behind dynamic light scattering is based on the Brownian motion of particles, which results in the fluctuation of scattered light intensity as the particles move. We have previously described for the first time the dynamics of the behavior of the DLS signal on a finger where blood flow was stopped [22]. We suggested that in the absence of blood flow, red blood cells gradually begin to behave like Brownian particles and the DLS signal reflects the dynamics of such particles. However, the assumption that erythrocyte aggregation influences signal kinetics was not validated in this study. Nevertheless, a marked change in DLS signal dynamics following the cessation of blood flow was observed.

The objective of this study was to investigate the relationship between the kinetics of the post-occlusion dynamic light scattering (DLS) signal and the rate of red blood cell (RBC) aggregation. Our hypothesis posited that changes in the DLS signal following occlusion would correspond to variations in RBC aggregation. To explore this hypothesis, we leveraged the observation that individuals with infectious diseases often exhibit heightened levels of RBC aggregation. Consequently, we compared the dynamics of the DLS post-occlusion signal obtained from a control group to those of hospitalized patients who had contracted COVID-19 or other infectious diseases. Notably, this study represents the first empirical examination of this hypothesis.

2. Theoretical consideration

2.1. DLS signal of aggregated RBC

This study investigates a new non-invasive approach to measure blood aggregation parameters using DLS. Building upon previous research [15,18], we apply the same methodology, albeit with a key difference: we analyze DLS signal response to the process. The methodology's fundamental principle remains unaltered: local blood flow is stopped to halt the action of shear forces that prevent the formation of significant aggregates during blood flow. Once the shear forces cease, the aggregation process begins, which is observable using the DLS signal. To describe this phenomenon using DLS, we must consider the following factors:

a) The process of red blood cell (RBC) aggregation leads to an enlargement of the scatterers, consequently causing a reduction in the particle diffusion coefficient. In the context of the Brownian motion scenario, this phenomenon can be captured using the conventional dynamic light scattering (DLS) approach. Notably, the spectral alteration in the DLS signal manifests within the low-frequency range.

b) The total measured energy of the DLS signal is driven by the mean size and concentration of the red blood cells and aggregates present at each moment in time.

Biomedical Optics EXPRESS

Let us assume a simplified situation where at least a part of the erythrocytes, immediately after the stoppage of blood flow, changes the mode of motion from laminar blood flow to near-Brownian motion. The Diffusion coefficient of the Brownian particle D_B is described by well-known Stokes-Einstein equation:

$$D_B = \frac{K_B T}{3\pi\eta d} \tag{1}$$

In our case T is blood temperature, η is plasma viscosity, d size of the particle, K_B – the Boltzmann constant.

The autocorrelation function of the DLS signal is connected to the diffusion coefficient of the moving particles through the following expression [21]:

$$ACF = \exp(-\Gamma\tau), \quad \Gamma = 2D_B q^2, \quad q = (4\pi n/\lambda)\sin(\theta/2), \tag{2}$$

Where n is refractive index of the blood plasma, λ - wavelength, θ is the angle between the incident light and the detection axis.

During the aggregation an average size of the particle increases. To assess the size of the aggregate we used expression from [20] where the aggregate is considered as composed of N_R erythrocytes (each with volume V_0). For a given size of small aggregates, an equivalent sphere with radius r_{eff} composed of N_R erythrocytes is given by:

$$r_{eff} = \left(\frac{3V_0 N_R(t)}{4\pi}\right)^{1/3}, \quad d = 2r_{eff}, \tag{3}$$

The expression (2) can be represented in terms of the power spectrum using the following formula [23]:

$$P(\omega) = \frac{2\Gamma}{\Gamma^2 + \omega^2} \tag{4}$$

Practically, to adjust (4) to experimentally obtained characteristics the frequency response $F(\omega)$ of the measurement must be taken into consideration. Therefore (4) is corrected by the following expression:

$$P(\omega) = \frac{2\Gamma}{\Gamma^2 + \omega^2} \cdot F(\omega) \tag{5}$$

By using (3) we can plot P(ω) (Fig. 1) for the single and double RBC for our experimental system (F(ω) is the high pass filter with cut-off 30 Hz).

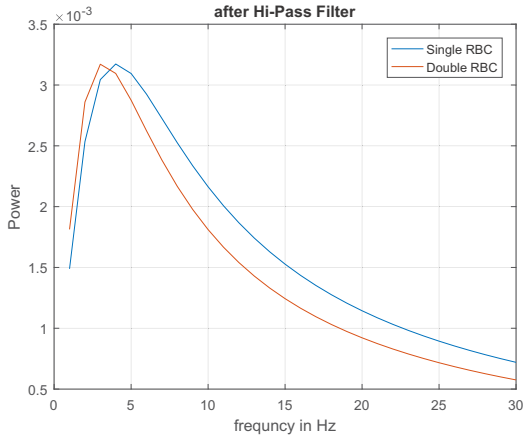

Fig. 1. Power as a function of frequency for single RBC and double RBC from (5)

Biomedical Optics EXPRESS

The equation governing rouleaux formation [24] expresses a linear relationship between time and the average number of cells per aggregate (NR) as a function of time and is represented by $N_R(t) \sim 1 + 0.5\upsilon Ht$, where v denotes the aggregation rate and H represents the hematocrit. We assume that at least at the beginning, that blood vessels facilitate the linear aggregation of RBCs. For sake of simplicity, we take that this $N_R(t)$ reaches the maximum value of 2. Therefore, we have modified this model by imposing a constraint that limits the aggregation process to create a rouleaux containing only two RBCs. Under this simplest scenario, where single erythrocytes combine to form double aggregates, N_R can be expressed as follows:

$$N_R(t) = 2 - \exp(-\upsilon Ht) \tag{6}$$

The Fig. 2 below exemplifies how the rate of N_R grows for two different values of υ=1.2 for fast and $\upsilon = 0.1$ for slow rate.

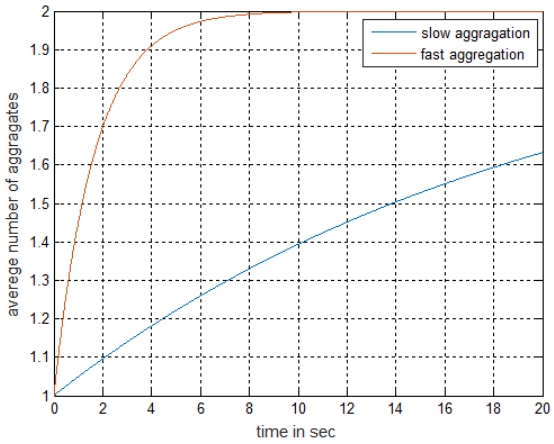

Fig. 2. The average number of cells per aggregate for two different rates of aggregation.

To enable a meaningful comparison between our model and experimental results, our aim is to describe the process in terms of kinetics. To achieve this, we will transform the spectral characteristics of the signal into an energy-based representation. More specifically, we will evaluate the integral of the total spectrum as a function of particle size, which varies over time. By using Eq. (5), we can determine the total energy measured by Dynamic Light Scattering (DLS):

$$EnF(\Gamma(t)) \approx \int \frac{2\Gamma(t)}{\Gamma^2(t) + \omega^2} \cdot F(\omega) d\omega \tag{7}$$

The Fig. 3 shows the behavior of normalized $EnF(\Gamma(t))$ for two cases "slow rate" and "fast rate":

2.2. Backscattering signal

In biological tissue, the reflected optical signal consists of two components: the static component, scattered from tissue, and a dynamic component associated with moving erythrocytes. Our focus is on the latter component, as it contributes to dynamic light scattering. Specifically, we study photons that interact with moving erythrocytes and are scattered back by 180 degrees, as this yields the maximum value of Γ (see eq 2).

In further modeling, we will consider only single scattering of light. The practical absence of the diffusive component is not obvious, and within the scope of this discussion, we can qualitatively justify this model as follows: Generally speaking, the photons that are scattered

Biomedical Optics EXPRESS

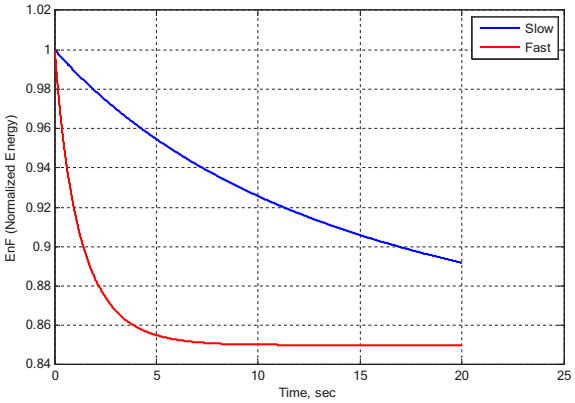

Fig. 3. Decay of normalized *EnF* as function of time.

by tissue and erythrocytes and reach the detector can be divided into three categories: Some photons penetrate deep into the tissue and undergo scattering processes. Scattering on a single red blood cell is characterized by a very narrow angular scattering diagram meaning that the angular deviation of the forward-scattered photon from its original path is very small [25]. Consequently, the Doppler frequency shift of these photons is also very small. Although these photons are scattered forward, they can still reach the detector even after a single forward-scattering event, by scattering backward from the tissue cells. As can be easily calculated, the Doppler shift of these scattered photons is found at frequencies below tenths of a hertz. These frequencies, which are filtered out by the analog filters of our receiving system, do not contribute to the measured spectrum of the detected signal. Now let's consider the photons that have "wandered" within the tissue and undergo multiple scattering events on erythrocytes. Due to the small scattering angles, these photons must undergo a long chain of scattering events in order to reach the back hemisphere. Indeed, these photons represent the diffusion component of light scattered by erythrocytes. However, due to their long trajectory within the tissue and blood, they return to a region quite far from the light source. This is precisely why in all reflection systems that specifically study the diffusion part of the signal, detectors are positioned as far away as possible from the light source. In our case, however, the detector is located in close proximity to the light source, resulting in an extremely low probability of diffusely scattered photons reaching the detector. And finally, there are photons that scatter directly back to the detector from erythrocytes. These photons represent single backscattering events. They exhibit the maximum Doppler shift, and that is why in the measurement system where the detector is located close to the light source, these photons make the main contribution to the measured spectrum. Their contribution to the measurable frequency range is dominant in shaping the spectrum being studied. Indeed, it can be said that our system is designed specifically to investigate the single back scattering of light from blood.

To calculate the backscattering cross-section from the single RBC or from the aggregate, we adopted a model of light scattering from an oblate spheroid [26]. Here, erythrocyte aggregation is described as a process of increasing in the minor axis of the spheroid. In this simplified model, the average aggregate size is grown by inflating the minor axis of the spheroid "c", while the major axis "a" remains unchanged. Additionally, the average density of the scatterers is inversely proportional to the volume of the scatterers.

For a single erythrocyte, the length c (1.1 microns) doubles when $N_R = 2$. It is important to note that N_R can take any value between 1 and 2, as it represents the average length of aggregates in the volume containing both single and double aggregates, with the statistical distribution

Biomedical Optics EXPRESS

between both types changing over time. To track the growth of this size over time, we examine how the value of "c" increases as N_R varies from 1 to 2.

$$c(t) = 1.1 \cdot N_R(t) \tag{8}$$

In this model, the aggregation process is characterized by the elongation of the small axis "c" of the oblate spheroid over time, which causes a change in the surface area and volume of the scattering particle. The surface area (S(t)) and volume (V(t)) of the newly created spheroids can be calculated using the following equations:

$$S(t) = 2\pi a^2 + \pi \frac{c(t)^2}{\varepsilon} ln \frac{1+\varepsilon}{1-\varepsilon}, \quad V(t) = \frac{4}{3}\pi a^2 c(t), \quad \varepsilon = \sqrt{1 - \frac{c(t)^2}{a^2}}, \tag{9}$$

The cross-section for single scattering of the spheroid σ_{bs} (t) towards the back hemisphere is proportional to its surface area [26];

$$\sigma_{bs} \sim S \tag{10}$$

The intensity of the backscattered light is directly proportional to the σ_{bs} (t) and to the density of the scatterers. The density of the ρ scattering particles is given by:

$$\rho(t) \sim 1/V(t) \tag{11}$$

Therefore, the total reflection (R_b) of the backscattered signal will be approximated by:

$$R_b(t) \sim S(t)/V(t) \tag{12}$$

As the volume of a spheroid grows faster than its surface area, the backscattered energy will decrease with the increase in the aggregation process. Equation (7) defines the entirety of optical energy, whereas $R_b(t)$ in Eq. (12) measures the fraction of signal that is backscattered by the red blood cells. Consequently, the total energy of the reflected light TE(t) is expressed as a product of total energy $EnF(t)$ by $R_b(t)$:

$$TE(t) \sim R_b(t) \cdot \int \frac{2\Gamma(t)}{\Gamma^2(t) + \omega^2} \cdot F(\omega) d\omega \tag{13}$$

From a practical perspective, TE(t) represents the total energy obtained from the current measured spectrum of the dynamic light scattering (DLS) signal. The graph below (Fig. 4) illustrates the decay of TE(t) over time for H = 0.5 and "slow and fast rate" of the aggregation as it was defined earlier in the text.

The main objective of the outlined model was to obtain a qualitative understanding of ongoing processes by analyzing the DLS signal during the initial stages of RBC aggregation that occur immediately after blood flow cessation. However, there are some simplifications in this model. One of the main assumptions is that the erythrocyte aggregation process does not continue beyond the formation of double aggregates, which is not entirely accurate. The rate and structure of RBC aggregation beyond double RBC are not solely defined by the initial kinetics. In fact, the continued growth of aggregates beyond small linear aggregates can evolve into a more complex, three-dimensional growth process [9]. This means that the assumptions made in the model about the cessation of erythrocyte aggregation after double aggregates were formed may not accurately represent the actual dynamics of the process. It is important to consider the more complex kinetics that can lead to the growth of larger and more complex RBC aggregates beyond the initial stages of aggregation. Furthermore, it is possible for both linear and volumetric growth of aggregates to occur simultaneously in different vessels. Additionally, the model did not consider

Biomedical Optics EXPRESS

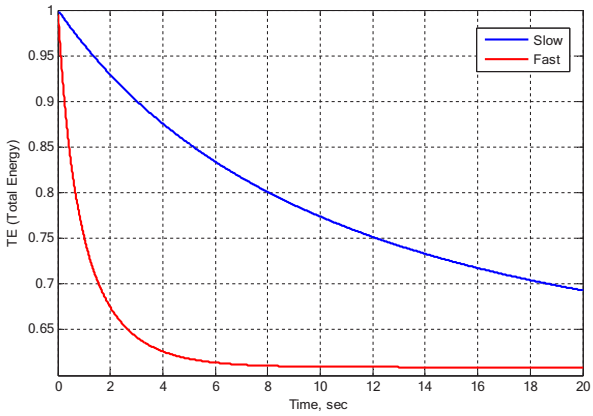

Fig. 4. Decay of the DLS spectrum energy due to the aggregation

the impact of local blood microflows associated with pressure gradients. This factor can cause a shift in the power spectral curve to higher frequencies.

It should be noted that we approximated the aggregates of erythrocytes using two different methods. When considering the diffusion of a Brownian particle, we employed a sphere approximation. However, for the calculation of light scattering, we utilized the spheroid approximation. This distinction in approximation methods stems from the different physical processes involved: particle diffusion and light scattering. This difference arises because light scattering is highly sensitive to shape, whereas Brownian diffusion is much less sensitive to shape.

To summarize, our simplified analysis suggests that the primary changes in the signal during the initial post-occlusion stage are linked to a decrease in the backscattered light and diffusion coefficient of the scatterers resulting from erythrocyte aggregation. Both of these effects contribute to a decrease in the energy of the DLS spectrum with time due to aggregation.

3. Experimental system and data collection

3.1. Measurement system and the finger probe

The measurement system comprises two so-called “mDLS” (Miniaturized Dynamic Light Scattering) sensors symmetrically positioned on opposite sides of the finger. Each” mDL” module consists of a laser light source (VCSEL) and two detectors, one on each side of the laser. The VCSEL illuminates the skin surface, and the reflected laser light is detected by the two sensors. The two signals are subtracted from each other and then passed through a differential amplifier. The resulting signal is digitized and stored in the computer’s memory at a sampling rate of 48KHz.

To ensure accurate measurements, the two “mDLS” modules are situated on the outer side of a transparent silicone inflatable ring that covers the skin surface at the root of the finger. This allows the reflected light to pass through the transparent silicone without any interference. Prior to measurement, air is pumped into the silicone ring to a pressure of 220 mmHg, which stops blood flow in the measurement area. Signal measurement on the two modules begins immediately after reaching 220 mm Hg. (Fig. 5).

3.2. Data collection protocol

In this study we collected data from three groups of subjects: healthy subjects, inflammation group and Covid-19 group. In the healthy control group, participants included hospitalized

Biomedical Optics EXPRESS

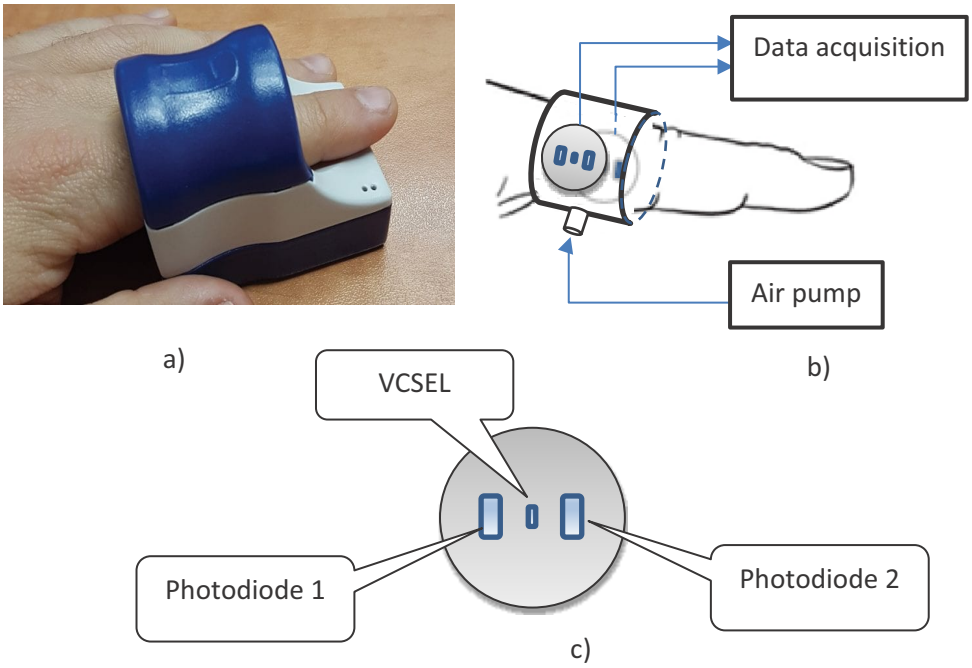

Fig. 5. **a)** The actual view of the probe. **b)** Schematic view of the measurement system. **c)** "mDLS" module.

patients without any inflammatory processes and non-hospitalized volunteers, The following inclusion criteria were selected for participant recruitment focusing on inflammatory processes: This included the patients admitted to hospital with bacterial pneumonia, autoimmune diseases, inflammatory bowel disease or based on laboratory analyses and clinical symptoms, were classified by their attending physician as suffering from severe inflammations. In the group of COVID-19 patients, hospitalized individuals with confirmed COVID-19 were included. These patients were admitted to the hospital due to the presence of COVID-19-related complications. All participants provided their informed consent to undergo measurements in accordance with the approved protocol of the ethics committee (Helsinki protocol). The age inclusion was: all subjects 18 years and older and able to sign informed consent. The exclusion criteria were for subjects unable to sign informed consent and pregnant women. The first group consisted of 65 healthy volunteers, while the second group comprised 34 hospitalized patients diagnosed with varying degrees of infection. The third group included 29 hospitalized patients who had developed various complications from COVID-19. To measure the subjects' signal using the measuring system, a sensor was positioned on one of their fingers while they were in a supine position. Subsequently, air was pumped into a pneumatic cuff wrapped around the finger, elevating the pressure to over 220 mm Hg, surpassing the systolic pressure. Following this, the VICSELs on two sensors were activated, and the sensors situated above the constricted area of the finger began recording the signal. The measurement process persisted for 60 seconds, after which the cuff's pressure was restored to its initial level. The captured signal was then subjected to analysis and further processing using a computer.

4. Results and discussion

We examined the temporal dynamics of total spectral energy for each group of subjects. Initially, we established a strong correlation in the behavior of the normalized total spectrum energy

Biomedical Optics EXPRESS

(TE) between the two channels, with an R value of 0.8 across 1351 data points. Consequently, subsequent analyses were conducted using measurements from a single channel. Figure 6 below depicts the average variation in total normalized energy over time for three groups: a control group and two patient groups.

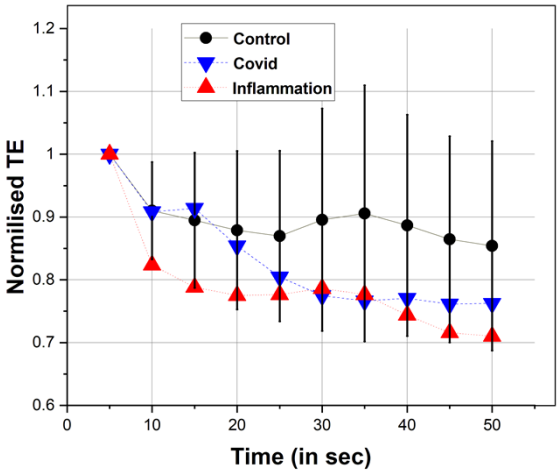

Fig. 6. Change of the normalized mean spectral energy (NTE) for 3 groups of subjects. The error bars depict the average deviation of each normalized value across time intervals within the cohort of 65 control subjects.

Based on our observations, there is a significant variation in the average rate of decline in spectral energy among the three groups under investigation. Notably, patients with COVID and infectious diseases exhibit the most rapid decrease, aligning with our initial expectations. These findings indicate that the rate of erythrocyte aggregation in the control group is notably slower compared to individuals with illnesses.

Furthermore, we attempted to detect differences at the individual level by creating a new index based on the energy drop dynamics of the DLS signal. The index NAI (Non-invasive Aggregation Index) was defined by the following expression:

$$NAI = a_0 + \sum_1^m a_i TE(t_i) \tag{14}$$

The indices correspond to specific time intervals captured during the measurement process. In our case m = 5, and the a_i coefficients are adjusted in such a way that the mean value of NAI for the control group will be zero ($p < 10^{-4}$). As can be seen a higher NAI indicates a higher rate of aggregation for the individual in question (Fig. 7(a), Fig. 7(b)). Higher NAI values correspond to a higher probability of belonging to groups with severe COVID or other infectious diseases.

The Table 1 provides the mean values and standard deviations of the variable NAI for three study groups

Table 1. Statistical distribution of NAI.

	Number of subjects	The mean value of NAI	Standard deviation
Control Group	65	-0.035	2.1
Inflammation	34	2.3	2.0
Covid	29	2,2	2,3

While there appears to be a significant similarity between the figure obtained through optical response modeling (Fig. 4) and the experimentally obtained results (Fig. 6), it is important to note

Biomedical Optics EXPRESS

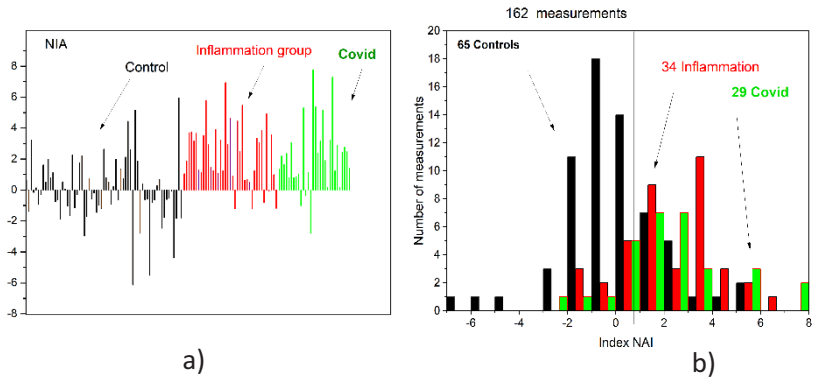

Fig. 7. **a)** Noninvasive Aggregation Indexes (NAI) for three group of subjects. **b)** Distribution of NAI for three group of subjects

that the theoretical post-occlusion behavior of the signal does not fully reflect all the phenomena that can occur *in vivo*. For instance, the model does not take into account erythrocyte interaction with vessel walls, blood flow from different vessels under pressure, changes in plasma viscosity, adhesion to other blood particles, and the complex distribution of aggregates between different vessels with sedimentation of erythrocytes on vessel walls. Despite the influence of numerous uncontrolled variables within the system, the optical signal arising from red blood cell aggregation remains remarkably potent. Even in the face of such complexity, the suggested simplistic model manages to adeptly capture the fundamental underlying dynamics of the aggregation process, yielding a compelling approximation of the experimental results. However, further research is needed to develop a more comprehensive model that can account for these additional factors and provide a more accurate representation of the process.

It should be noted that to date, there is no unified standard for measuring the tendency of aggregation, even *in vitro*. Furthermore, the process of aggregation in blood vessels can significantly differ from the aggregation process observed *in vitro*, as the one-dimensional aggregation process that likely predominates in narrow vessels may follow different kinetic laws than the three-dimensional aggregation measured *in vitro*. Aggregation in blood vessels can be influenced not only by geometric factors limiting aggregate growth but also by interactions with the endothelium, which also affect the mobility of red blood cells. Hence, the advancement of non-invasive aggregation measurement techniques should not rely solely on correlation with existing methods. Instead, it should be regarded as an independent methodology with its own clinical and physiological significance. The obtained results indirectly validate the role of the RBC aggregation process in the DLS signal and highlight the potential clinical significance of this non-invasive approach in detecting the onset of infectious or inflammatory diseases. To further improve the measurement methodology, it is viable to employ a system with detectors placed at greater distances from the light source to effectively manage the diffuse component of the signal. Furthermore, while it may add some complexity to the system, conducting measurements simultaneously on two fingers offers advantages, as the observed effect should not depend on the specific measurement location. Regarding the validation of the proposed non-invasive methodology, future techniques such as capillaroscopy can be utilized. Additionally, employing a clinical model associated with the study of inflammatory processes seems to be the most effective approach for investigating red blood cell aggregation.

In summary, non-invasive measurement of RBC aggregation holds great potential in providing crucial diagnostic information for the early detection and management of inflammation. These measurements can serve as early indicators for cardiovascular disease, stroke, and other related

Biomedical Optics EXPRESS

conditions. By offering early warning signs, they enable healthcare professionals to take proactive measures and administer appropriate treatments to patients. It is worth highlighting that the simplicity of the proposed measurement approach allows for its convenient application in ambulatory settings or home care. This contributes to the advancement of personalized medicine and facilitates home self-monitoring of health, promoting greater patient involvement in their own well-being.

Funding. Elfi-Tech Ltd.

Disclosures. The authors have no relevant financial interests in the manuscript and no other potential conflicts of interest.

Data Availability. Raw data used in this study are available from the corresponding author upon request.

References

1. O. K. Baskurt and H. J. Meiselman, "Erythrocyte aggregation: basic aspects and clinical importance," Clin. Hemorheol. Microcirc. **53**(1-2), 23–37 (2013).
2. X. I. Weng, G. Cloutier, R. A. Beaulieu, and G. O. Roederer, "Influence of acute-phase proteins on erythrocyte aggregation," Am. J. Phys.-Heart and Circulatory Phys. **271**(6), H2346–H2352 (1996).
3. R. Ben Ami, G. Friedman, Y. Schwammenthal, J. Kadar, A. Hofman, and G. Keren, "Parameters of red blood cell aggregation as correlates of the inflammatory state," Am. J. Phys.-Heart and Circulatory Phys. **280**(5), H1982–H1988 (2001).
4. W. H. Reinhart, A. Singh, and P. W. Straub, "Red blood cell aggregation and sedimentation: the role of the cell shape," Br. J. Haematol. **73**(4), 551–556 (1989).
5. S. Crowson Cynthia, M. U. Rahman, and E. L. Matteson, "Which measure of inflammation to use? A comparison of erythrocyte sedimentation rate and C-reactive protein measurements from randomized clinical trials of golimumab in rheumatoid arthritis," The J. Rheumatol. **36**(8), 1606–1610 (2009).
6. S. E. Bedell and B. T. Bush, "Erythrocyte sedimentation rate: from folklore to facts," The Am. J. Med. **78**(6), 1001–1009 (1985).
7. G. Fusman, C. Moretti, T. Borchers, and M. Lombardi, "Red blood cell adhesiveness/aggregation, C-reactive protein, fibrinogen, and erythrocyte sedimentation rate in healthy adults and in those with atherosclerotic risk factors," Am. J. Cardiol. **90**(5), 561–563 (2002).
8. E. Nader, R. Ortega, M. Vernet, H. Dupont, and J. L. Hanouz, "Increased blood viscosity and red blood cell aggregation in patients with COVID-19," Am. J. Hematol. **97**(3), 283–292 (2022).
9. M. Higuchi and N. Watanabe, "A rapid and accurate method for estimating the erythrocyte sedimentation rate using a hematocrit-corrected optical aggregation index," PLos One **17**(7), e0270977 (2022).
10. C. V. L. Pop and S. Neamtu, "Aggregation of red blood cells in suspension: study by light-scattering technique at small angles," J. Biomed. Opt. **13**(4), 041308 (2008).
11. S. V. Tsinopoulos, E. J. Sellountos, and D. Polyzos, "Light scattering by aggregated red blood cells," Appl. Opt. **41**(7), 1408–1417 (2002).
12. M. Donner, M. Siadat, and J. F. Stoltz, "Erythrocyte aggregation: approach by light scattering determination," Biorheology **25**(1-2), 367–376 (1988).
13. M. R. Hardeman, J. G. G. Dobbe, and C. Ince, "The Laser-assisted Optical Rotational Cell Analyzer (LORCA) as red blood cell aggregometer," Clin. Hemorheol. Microcirc. **25**(1), 1–11 (2001).
14. I. Gurov, M. Volkov, and N. Margaryants, *et al.*, "High-speed video capillaroscopy method for imaging and evaluation of moving red blood cells," Opt. Lasers Eng. **104**, 244–251 (2018).
15. I. Fine, B. Fikhte, and L. D. Shvartsman, "RBC-aggregation-assisted light transmission through blood and occlusion oximetry," Proc. SPIE **4162**, 130–139 (2000).
16. I. Fine and A. Kaminsky, "Possible error in reflection pulse oximeter readings as a result of applied pressure," J. Healthcare Eng. **2019**(1), 1–7 (2019).
17. I. Fine and A. Kaminsky, "Scattering-driven PPG signal model," Biomed. Opt. Express **13**(4), 2286–2298 (2022).
18. I. Fine, B. Fikhte, and L. D. Shvartsman, "Occlusion spectroscopy as a new paradigm for non-invasive blood measurements," Proc. SPIE **4263**, 122–130 (2001).
19. M. P. McEwen and K. J. Reynolds, "Light transmission patterns in occluded tissue: Does rouleaux formation play a role?" Proc. World Congress Eng. **1**, WCE (2012).
20. L. D. Shvartsman and I. Fine, "Optical transmission of blood: Effect of erythrocyte aggregation," IEEE Trans. Biomed. Eng. **50**(8), 1026–1033 (2003).
21. J. Stetefeld, S. A. McKenna, and T. R. Patel, "Dynamic light scattering: A practical guide and applications in biomedical sciences," Biophys. Rev. **8**(4), 409–427 (2016).
22. I. Fine and A. Kaminsky, "In vivo dynamic light scattering measurements of red blood cell aggregation," Proc. SPIE **6436**, 64360C (2007).
23. B. Chu, *Laser Light Scattering: Basic Principles and Practice* (Courier Corporation, 2007).

Biomedical Optics EXPRESS

24. G. Barshtein, D. Wajnblum, and S. Yedgar, "Kinetics of linear rouleaux formation studied by visual monitoring of red cell dynamic organization," Biophys. J. **78**(5), 2470–2474 (2000).
25. M. Hammer, D. Schweitzer, B. Michel, E. Thamm, and A. Kolb, "Single scattering by red blood cells," Appl. Opt. **37**(31), 7410–7418 (1998).
26. V. Twersky, "Absorption and multiple scattering by biological suspensions," J. Opt. Soc. Am. **60**(8), 1084–1093 (1970).